About frequency properties of solar-like stars

Janine Provost
OCA, dept Cassini-UMR CNRS 6529, 06304 Nice Cedex 4, France

ABSTRACT

In the context of the preparation for COROT, we have studied some theoretical properties of the frequencies of solar-like stars. In order to prepare the interpretation of future data, we have defined between Meudon (DASGAL) and Nice (Cassini) a hare and hounds exercise as follows: from a set of frequencies provided by each group to the other, find the characteristics of the corresponding stellar model. Here are reported preliminary results obtained by the Nice group. A discussion on the numerical accuracy of theoretical frequencies is also given.

1. Introduction

In order to prepare the interpretation of future observations of COROT, specially for solar like stars, an hare and hounds exercise has been decided between a Nice (Cassini) group [1] and a Meudon (DASGAL) group [2]. The aim is to find the main characteristics of an unknown stellar model from a set of frequencies provided by the other group (referred to as exercise frequency set). The stellar model has to be in a given box of HR diagram. In that aim we have studied the properties of solar like oscillation frequencies for stellar models inside this box. Here we present the properties of these frequencies and we report the preliminary results obtained by the Nice group from frequencies sent by the Meudon group. To put constraints on the structure of stellar interiors by asteroseismology and to fully exploit the future observations of COROT, one has to modelize the stellar structure and oscillations as accurately as possible. Here the accuracy of the frequencies of oscillations is also discussed.

First, I define the hare and hounds exercise and present the stellar models computed for it (section 2). Next I discuss the accuracy and some properties of the stellar frequencies (sections 3 and 4). Finally we present the results and preliminary conclusions of the exercise (section 5).

2. Hare and hounds exercise - stellar models

We decided to mimic observed frequencies corresponding to observations in a given box of luminosity and effective temperature:

$$0.83 \leq \log L/L_{\odot} \leq 0.89$$

[1] Nice group: G. Berthomieu, T. Corbard, G. Gonczi, P. Morel, J. Provost, T. Toutain

[2] Meudon group: C. Barban, M.J. Goupil, Y. Lebreton, E. Michel, I. Roxburgh

$$6400\mathrm{K} \leq T_{\mathrm{eff}} \leq 6600\mathrm{K} \quad (3.806 \leq \log T_{\mathrm{eff}} \leq 3.819)$$

We restrict the parameters describing the convection, the mixing-length parameter λ and the overshoot core parameter ζ, to the following realistic range:

$$1.55 \leq \lambda \leq 1.85 \quad 0 \leq \zeta \leq 0.3$$

As a first step, we suppose that the chemical abundances are known:

$$Z = 0.02, \qquad Y = 0.28$$

The corresponding metallicity is $Z/X = 0.0286$, i.e. larger than the solar value $Z/X = 0.0245$.

We assume that we know the frequencies of all the identified modes in the following frequency range:

$$\nu \geq 300\mu\mathrm{Hz} \ \text{ for } \ \ell = 0, 1;$$

$$\nu \geq 400\mu\mathrm{Hz} \ \text{ for } \ \ell = 2, 3.$$

We have computed with the CESAM code (Morel 1997) about 40 models satisfying the above prescriptions, with a given physics: nuclear data from Caughlan & Fowler (1988), EFF equation of state (Eggleton et al. 1973), OPAL opacities (routine from Y. Lebreton), Eddington law for the atmosphere description (see Morel et al. 1994). The microscopic diffusion is neglected. Most of the models are computed with a small constant turbulent mixing.

The global characteristics of the models are given in Table 1. Their evolutionary tracks in the HR diagram are plotted in Fig. 1 and Fig. 2. All the models are in hydrogen burning phase, except model A in post main sequence phase and model O which is finishing to burn its central hydrogen at a stage of increasing T_{eff}.

3. Oscillations - Numerical accuracy

Adiabatic oscillation frequencies $\nu_{n,\ell}$ depend on the variation along the radius r of the sound speed $c(r)$ and Brunt-Väisälä frequency $N(r)$ (n and ℓ are respectively the radial order and degree of the oscillation). The high frequency modes are mainly influenced by the sound speed and the low frequency ones depend also on the Brunt-Väisälä frequency. For solar-like stars with mass larger than the solar one, numerical problems may appear when computing $N(r)$, in the stage where the convective core decreases in size. This is due to the variation of chemical composition, which is constant in the convective core and which gradient has some bumps outside this core. Figure 3 (left panel) shows that it is the case for a model without any mixing or microscopic diffusion. For a model computed with a small constant turbulent mixing the, $N(r)$ profile is generally smoother (figure 4, left panel), except just at the frontier between convective and radiative zone where peaks may appear (figure 5, left panel). Model of Fig. 4 will be referred to as smooth model.

Table 1: Global characteristics of the stellar models. All models except A, D, E, are computed with a small constant turbulent mixing; models with λ=1 are computed with Canuto-Mazzitelli description of the convection; •• indicates that the model has a Ω_g value close to that of the unknown model ($\Omega_g = \sqrt{GM/R^3}$); $\overline{\Delta\nu}$ is the asymptotic mean large spacing of p mode spectrum $\overline{\Delta\nu} = 1/(2\int_0^R dr/c)$.

Name	λ	ζ	M/M$_\odot$	age (10^9yr)	X$_c$	$\log L/L_\odot$	$\log T_{\rm eff}$	$\overline{\Delta\nu}$ (μHz)
A	1.7	0.0	1.450	2.500	~ 0	0.88225	3.8107	50.65
C	1.7	0.2	1.500	2.200	0.225	0.82611	3.8073	55.49
C1 ••	1.7	0.3	1.500	2.200	0.300	0.83857	3.8139	56.46
D	1.7	0.2	1.525	2.100	0.222	0.85665	3.8089	53.55
E	1.7	0.2	1.525	2.150	0.203	0.85848	3.8061	52.52
E1 ••	1.7	0.1	1.525	1.920	0.200	0.83403	3.8117	56.57
E2 ••	1.7	0.2	1.525	1.950	0.275	0.85041	3.8164	56.56
F	1.7	0.2	1.530	2.000	0.251	0.85887	3.8136	54.92
H	1.7	0.2	1.530	2.000	0.251	0.85902	3.8136	54.89
H1 ••	1.7	0.2	1.530	1.920	0.279	0.85584	3.8174	56.44
H2	1.7	0.2	1.530	2.000	0.215	0.86451	3.8081	52.68
I ••	1.7	0.15	1.530	1.900	0.246	0.84834	3.8153	56.46
J	1.7	0.1	1.530	2.000	0.162	0.84254	3.8073	54.42
	1.7	0.1	1.530	1.780	0.249	0.83583	3.8184	58.72
L ••	1.7	0.1	1.530	1.900	0.206	0.84002	3.8129	56.46
L1.8 ••	1.8	0.1	1.530	1.930	0.188	0.84066	3.8131	56.72
L1.6 ••	1.6	0.1	1.530	1.850	0.229	0.83832	3.8135	56.57
M	1.0	0.1	1.530	1.839	0.221	0.83795	3.8143	56.98
M1 ••	1.0	0.1	1.530	1.870	0.213	0.83899	3.8133	56.57
N	1.0	0.1	1.530	1.900	0.196	0.83990	3.8112	55.82
N1	1.7	0.05	1.530	1.900	0.142	0.8297	3.8091	56.19
O	1.7	0.0	1.530	2.000	0.010	0.86761	3.8136	54.07
P ••	1.7	0.0	1.540	1.800	0.111	0.83185	3.8109	56.74
P1 ••	1.7	0.05	1.540	1.800	0.171	0.83994	3.8131	56.71
Q	1.7	0.10	1.540	1.800	0.226	0.84954	3.8164	56.87
Q+ ••	1.7	0.10	1.540	1.825	0.221	0.85060	3.8158	56.57
Q1 ••	1.7	0.15	1.540	1.820	0.262	0.85814	3.8185	56.71
R	1.7	0.0	1.550	1.800	0.095	0.84515	3.8100	55.34
R-	1.7	0.0	1.550	1.700	0.151	0.84183	3.8153	57.40
R- -	1.7	0.0	1.550	1.750	0.124	0.84317	3.8126	56.37
R1 ••	1.7	0.0	1.550	1.740	0.129	0.84287	3.8131	56.58
S	1.5	0.0	1.570	1.616	0.151	0.86324	3.8129	54.35
S1 ••	1.5	0.0	1.570	1.560	0.185	0.86187	3.8170	55.75
U	1.5	0.0	1.590	1.597	0.137	0.88807	3.8126	52.29
V	1.7	0.0	1.590	1.597	0.133	0.88775	3.8170	54.19
W	1.85	0.0	1.590	1.597	0.130	0.88707	3.8203	55.67

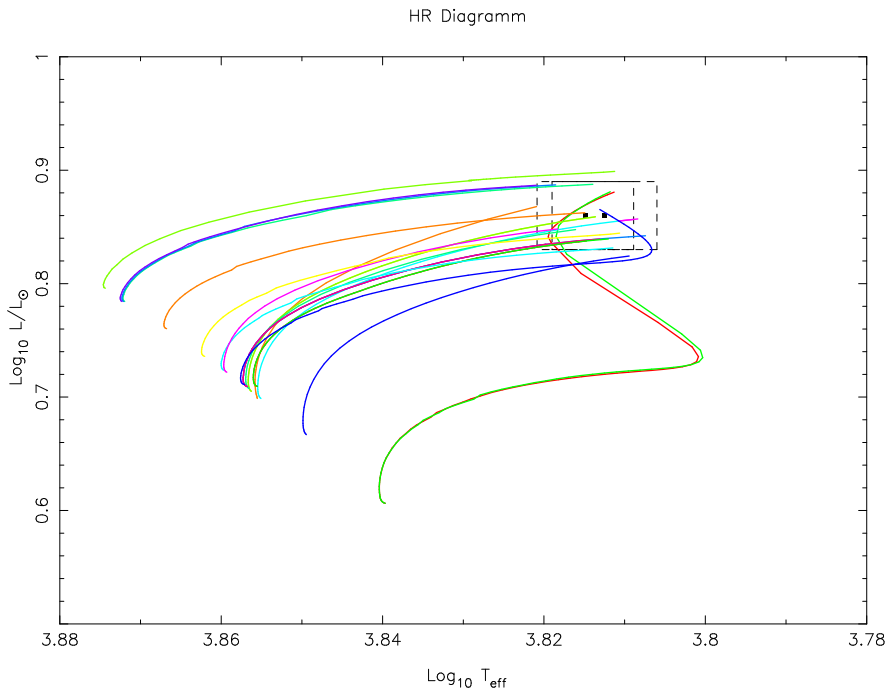

Fig. 1.— HR diagram: evolutionary tracks of the stellar models. The dashed error boxes correspond respectively to the hare and hounds exercise (right) and to Procyon (left, from Barban et al. 1999)

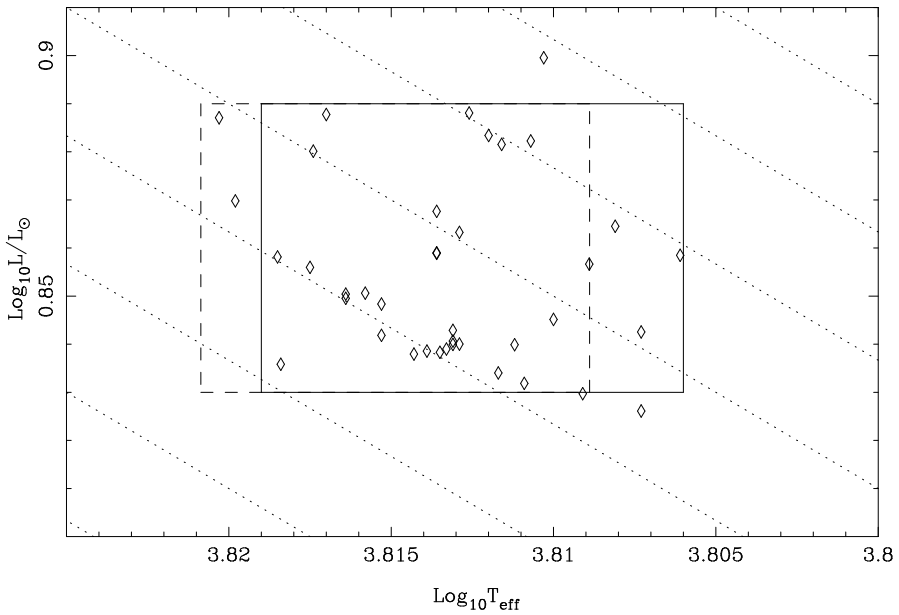

Fig. 2.— Position of the models in HR diagram. For the error boxes, same as in Fig. 1. The dotted lines represent lines of constant radius. For a star of given mass, they are also lines of constant dynamical frequency Ω_g.From one line to the next towards the right, the variation of the radius induces a decrease of Ω_g by about 2%.

To test the consequence of this problem and also the internal consistency of the models, we have computed the frequencies, using different sets of variables. Small frequency differences are expected if the consistency of the model is high enough and if the system governing the oscillations are accurately solved. Our oscillation code (Nice 1) uses, as in Unno et al. (1989), variables proportional to:

$$\xi_r,\ p',\ \Phi',\ \frac{d}{dr}\Phi', \qquad \text{(Nice1)}$$

where ξ_r is the radial displacement, p' the Eulerian pressure perturbation and Φ' the Eulerian perturbation of the gravitational potential. We have developed a new code (Nice 2) which avoids the use of N. It uses the following variables, similar to the one of Zharkov & Vorontsov (1989):

$$\xi_r,\ \delta p,\ \Phi',\ (\frac{d}{dr}\Phi' - 4\pi G\rho\xi_r). \qquad \text{(Nice2)}$$

δp is the Lagrangian perturbation of the pressure, ρ the density and G the gravitational constant. The last variables $(\frac{d}{dr}\Phi' - 4\pi G\rho\xi_r)$ is zero for radial modes.

We have also compared our results for a smooth model with the code QMW (Roxburgh & Vorontsov 2000)

$$\xi_r,\ p',\ \Phi',\ (\frac{d}{dr}\Phi' - 4\pi G\rho\xi_r). \qquad \text{(QMW)}$$

3.1. Comparison between the codes Nice1 and Nice2

We have compared the two codes Nice1 and Nice2 for some of our models. Results are given in right panels of Fig. 3, 4 and 5. The frequency differences

$$\delta\nu^{21}_{n,\ell} = \nu^{\rm Nice2}_{n,\ell} - \nu^{\rm Nice1}_{n,\ell}$$

are given for the models represented by their Brunt-Väisälä frequency in the left part of each figure. As expected, the most affected modes are the modes sensitive to Brunt-Väisälä frequency, i.e. the low frequency and mixed modes. Their frequencies depend on the code used and are changed by a few μHz. The radial modes frequencies are changed by 1 μHz for model D and by 0.1 μHz for the smooth model. This will induce changes in the small frequency separation between modes of degree ℓ=0 and 2 by the same amount. Note that for the smooth model the frequency differences are smaller by a factor 10 than for the model D. This may indicate also that the Brunt-Väisälä consistency of the smooth model is much better than the one of model D.

Even for models including some turbulent mixing, the limit between convective core and the radiative inner part may be difficult to localize. Figure 5 shows an example with a well-pronounced peak for the $N(r)$ profile. The corresponding frequency differences between results of Nice1 and Nice2 are quite large, particularly of order 1μHz for radial modes. If one removes "by hand" the peak, one obtains unchanged results for Nice2 and $\delta\nu^{21}_{n,\ell}$ is very much smaller.

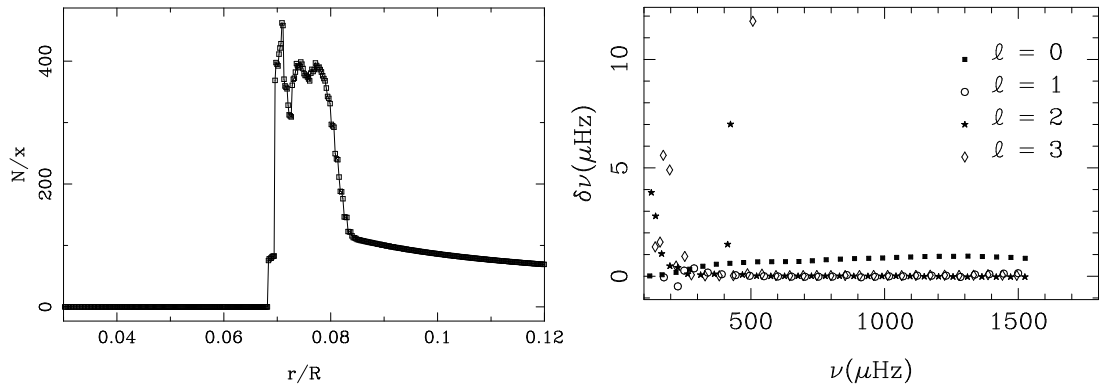

Fig. 3.— Left panel: Brunt-Väisälä frequency $N(r)$ divided by radius (dimensionless units) in the central part, for model D (M=1.525, Xc=0.222). Right panel: corresponding frequency differences $\delta\nu^{21}_{n,\ell} = \nu^{\rm Nice2}_{n,\ell} - \nu^{\rm Nice1}_{n,\ell}$.

In conclusion, as the problems in Brunt-Väisälä frequency profile which may occur are purely numerical and do not influence the structure in pressure, temperature and density of the model itself, it seems better to compute the stellar oscillation with the Nice2 code.

3.2. Comparison of QWM code with Nice codes

The comparison between QMW code and Nice1 and 2 codes has been made for the smooth model of Fig. 4. The frequency differences, given in Fig. 6, are rather small. Nice1 and QMW codes are in better agreement by a factor 2 than Nice2 and QMW. The most affected modes are low frequency modes and mixed modes. For radial modes Nice1 and QMW codes give very close results, the difference between Nice2 and QMW being of order $0.1\,\mu$Hz. The agreement for nonradial p modes of frequency larger than 500μHz is even better.

4. Oscillations - Frequency properties

4.1. Direct comparison of frequencies between model and exercise

In order to infer some information about the structure of the unknown model, we have computed the oscillations of all our models with the Nice2 code and we have made direct comparisons between these frequencies and the frequencies of the exercise. The relative frequency differences $\delta\nu/\nu$ of p mode oscillations between two models are such that:

$$\frac{\delta\nu_{n,\ell}}{\nu_{n,\ell}} = \frac{\delta\Omega_g}{\Omega_g} + (\frac{\delta\overline{\nu}_{n,\ell}}{\overline{\nu}_{n,\ell}}),$$

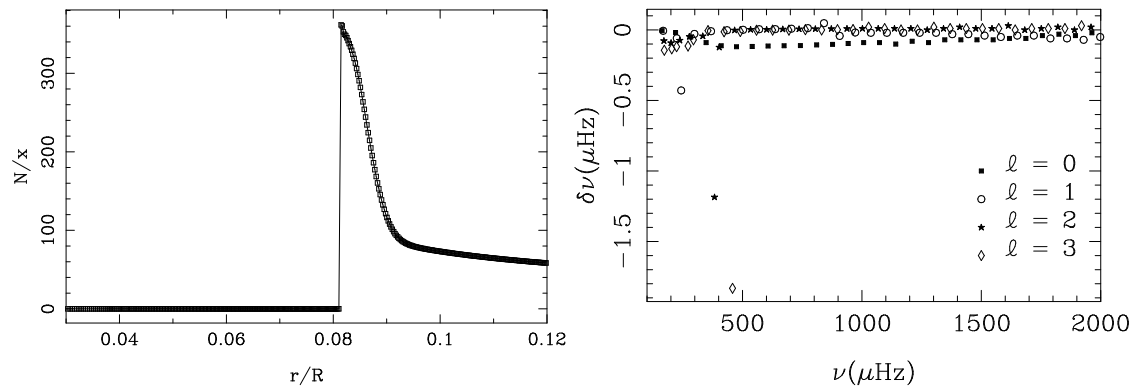

Fig. 4.— Same as Fig. 3 for a smooth model, with M/M$_\odot$=1.45, computed with a small constant turbulent mixing. Note that for this smooth model, $\delta\nu^{21}_{n,\ell}$ is smaller by factor 10 than for model D.

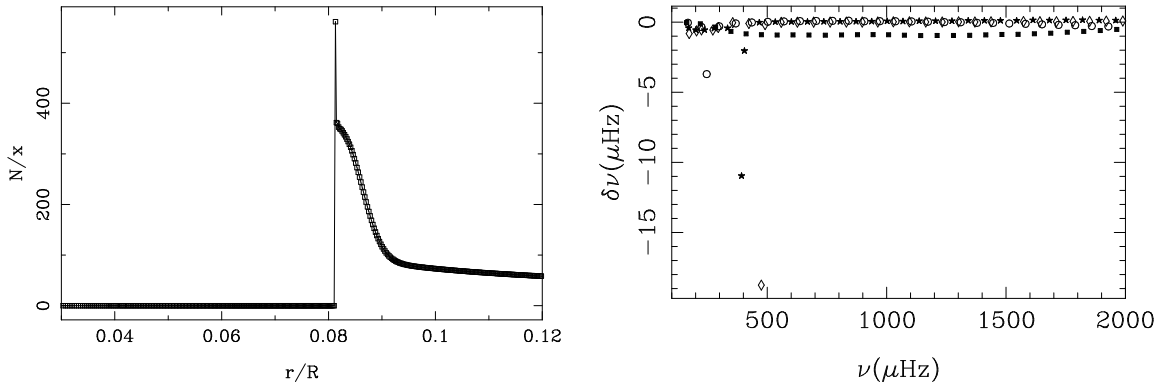

Fig. 5.— Same as Fig. 3 for a model,with M/M$_\odot$=1.45, computed with a small constant turbulent mixing, which has a peak at the upper limit of the convective core. Same symbols for the degrees ℓ as in Fig. 4

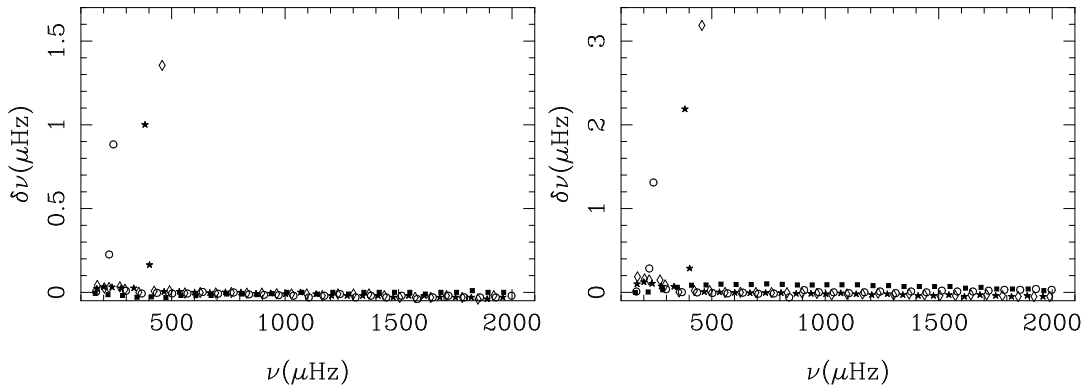

Fig. 6.— Frequency differences between QMW and Nice codes, for a smooth model (cf. Fig. 4, right panel). Left panel: QMW - Nice1, right panel: QMW - Nice2 . Same symbols for the degrees ℓ as in Fig. 4. The largest differences occur for mixed modes ($\ell = 1$, $n = 2$), ($\ell = 2$, $n = 3$) and ($\ell = 3$, $n = 4$).

where Ω_g is the dynamical frequency ($\Omega_g = \sqrt{GM/R^3}$) and $\overline{\nu}_{n,\ell}$ is the frequency normalized by Ω_g. An example is given in Fig. 7 which represents the differences between models L et D. The first term $\delta\Omega_g/\Omega_g$ is due to differences in mass and mainly in radius, and it generally dominates. In order to make inversions we will specially search for models with frequencies as close as possible to the frequencies of the exercise, hence with Ω_g as close as possible to that of the unknown model.

The second term corresponds to nonhomological differences of structure between the two models. It can have oscillatory behavior, well visible in Fig. 7. This may be due to the oscillatory components of the frequencies of each model, caused by the rapid variations of the stellar structure (see section 4.3).

4.2. Global characteristics from frequency separations

Several combinations of frequency of low degree p-modes inform us on different parts of the stellar structure. The large separation $\Delta\nu_{n,\ell}$ between the frequency of modes of given degree ℓ and consecutive radial orders,

$$\Delta\nu_{n,\ell} = \nu_{n,\ell} - \nu_{n-\ell},$$

depends on the external layers and is mainly related to the stellar radius or to Ω_g. It is roughly approximated by its asymptotic value $\overline{\Delta\nu}$ (see Table 1).

The small separations between frequencies of modes with degree $\ell, \ell+2$ or $\ell, \ell+1$, which penetrate differently in the central layers, are mainly sensitive to the stellar core:

$$\delta\nu_{\ell,\ell+2} = \nu_{n+1,\ell} - \nu_{n,\ell+2}$$

$$\delta\nu_{\ell,\ell+1} = 2\nu_{n,\ell} - (\nu_{n,\ell+1} - \nu_{n-1,\ell+1})$$

The second order differences

$$\delta^2\nu_{n,\ell} = \nu_{n,\ell} - 2\nu_{n+1,\ell} + \nu_{n+2,\ell}$$

depend on the external layers, specially the He ionization zone and the base of the convection zone (e.g. Gough 1991). All these frequency differences are given as function of the frequency in Fig. 8 for one model (model E1) and in Fig. 9 for the frequencies of the exercise.

In the high frequency range, the p-mode spectrum can be characterized by the mean of large and small frequency separations, usually estimated by analytical fits of the frequencies and of the small frequency separations. The numerical frequencies are fitted by the following polynomial expression (Berthomieu et al. 1993):

$$\nu_{n,\ell} = \nu_{0\ell} + \Delta\nu_\ell(n + \frac{\ell}{2} - n_0) + a_\ell(n + \frac{\ell}{2} - n_0)^2.$$

The quantities $\delta\nu_{\ell,\ell+2}$ and $\delta\nu_{\ell,\ell+1}$ vary almost linearly with the frequency or the radial order. Mean small spacings $\overline{\delta\nu}_{\ell,\ell+i}$ are estimated by using the following linear fit:

$$\delta\nu_{\ell,\ell+i} \sim \overline{\delta\nu}_{\ell,\ell+i} + S_{\ell,\ell+i}(n - n_0) \quad (i = 1, 2).$$

As in the solar case, we consider a set of 9 modes centered at $n_0 \sim 21$. ($n_{\rm min}$=17, $n_{\rm max}$=26, $\ell = 0$,1; $n_{\rm min}$=15, $n_{\rm max}$=25, $\ell = 2$, 3). The mean large spacing $\Delta\nu_0$ and the mean small spacings $\overline{\delta\nu}_{0,1}$, $\overline{\delta\nu}_{0,2}$ and $\overline{\delta\nu}_{1,3}$ have been estimated for all the models and for the exercise frequency set. Note that the mean large spacing $\Delta\nu_\ell$ does not depend much on the degree and that it is always smaller by 0.5 μHz than the asymptotic value $\overline{\Delta\nu}$ given in Table 1.

4.3. Effect of rapid variations in stellar structure

Rapid variations in stellar structure located at $r_{\rm rap}$ induce oscillatory behavior of the frequencies of p modes, with a "period" equal to the inverse of twice the travel time of the sound from the surface to the location of rapid variation (e.g. Gough 1991):

$$\mathcal{P}^{-1} = 2 \int_{r_{\rm rap}}^{R_*} \frac{dr}{c}.$$

Such rapid variations can occur at the limit of the convective core, at the base of the convection zone and at the HeII ionisation zone. This oscillatory behavior can be seen in some frequency separations. $\delta^2\nu_{n,\ell}$ has a sinusoidal behavior with two different "periods" of order 150 μHz and 370 μHz, as illustrated in Fig. 8 and Fig. 9. The lower period is due to a discontinuity in the derivative of the sound velocity at the base of the convection zone. The larger period has the largest amplitude and is due to the variation of the adiabatic index Γ_1 in the HeII ionization zone. Its measurement can provide an estimation of the depth of the HeII ionisation zone, hence give an information on the mixing-length value. This large period is also visible in the variation of $\Delta\nu_{n,\ell}$ with the frequency. The rapid variation of the sound speed at the frontier of the convective core gives rise to a much longer period (e.g. Audard & Provost 1994), i.e. from 2500 to 3500 μHz for the set of considered models. Thus it cannot be observed from frequency differences of a given model directly.

The oscillatory behavior of $\delta\nu/\nu$, well visible in Fig. 7 may be due to the oscillatory components of the frequencies of each model. For models D and L the rapid variations of the stellar structure at the limit of the convective core, at the base of the convection zone and at the HeII ionisation zone give rise respectively to the following values of $\mathcal{P}$: 2731 μHz, 141 μHz, 337 μHz, for model D and: 3000 μHz, 157 μHz, 370 μHz, for model L. Thus possible observable "periods" in frequency differences are: (3000-2730)/2, (337+370)/2, (141+157)/2, the other possibilities are either too small or too long.

5. Results and preliminary conclusions

We have estimated the mean large and small spacings for all the models and for the exercise frequency set: $\Delta\nu_0 = 56.1\mu$Hz, $\overline{\delta\nu}_{0,1} = 5.78\mu$Hz $\overline{\delta\nu}_{0,2} = 3.75\mu$Hz and $\overline{\delta\nu}_{1,3} = 5.85\mu$Hz. Using all the models computed within the error box in HR diagram, we have made several plots (Fig. 10 and Fig. 11) which show the following properties:

As expected the mean large spacing $\Delta\nu_0$ is a linear function of Ω_g. Thus it gives a measure of the mean stellar

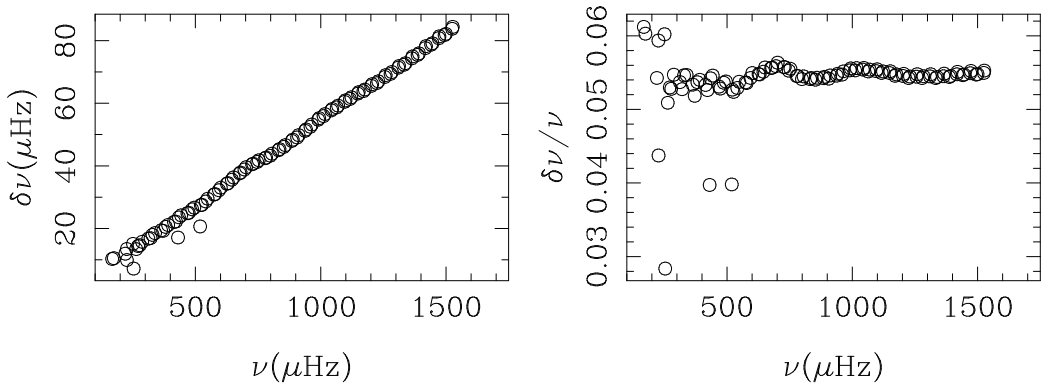

Fig. 7.— Frequency differences for modes of degree ℓ= 0 to 3, between models L and D. Left panel: $\delta\nu_{n,\ell}$, right panel $\delta\nu_{n,\ell}/\nu_{n,\ell}$. $\delta\nu_{n,\ell}$ varies almost linearly with $\nu_{n,\ell}$ with a slope close to $\delta\Omega_g/\Omega_g$(∼5.5%). The contribution of this term dominates the frequency differences. An oscillation with "period" around 350 μHz, corresponding to half sum of oscillatory components to the frequency of each model due to HeII ionisation zone, is well visible.

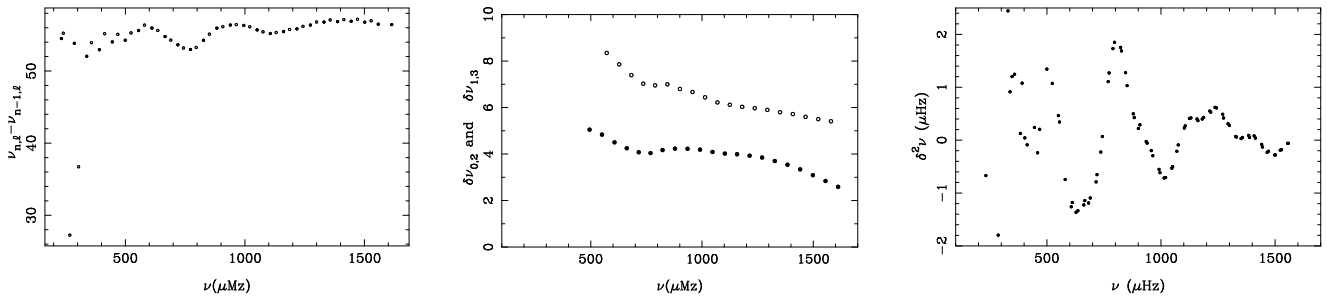

Fig. 8.— Frequency separations $\Delta\nu_{n,\ell}$, $\delta\nu_{\ell,\ell+2}$ for ℓ=0 and 2 and $\delta^2\nu_{n,\ell}$ for model E1.

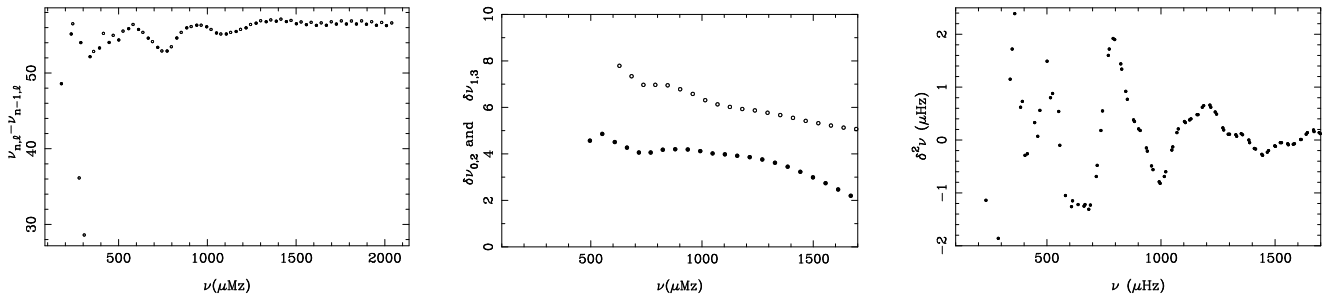

Fig. 9.— Frequency separations $\Delta\nu_{n,\ell}$, $\delta\nu_{\ell,\ell+2}$ for ℓ=0 and 2 and $\delta^2\nu_{n,\ell}$ for the exercise frequency set.

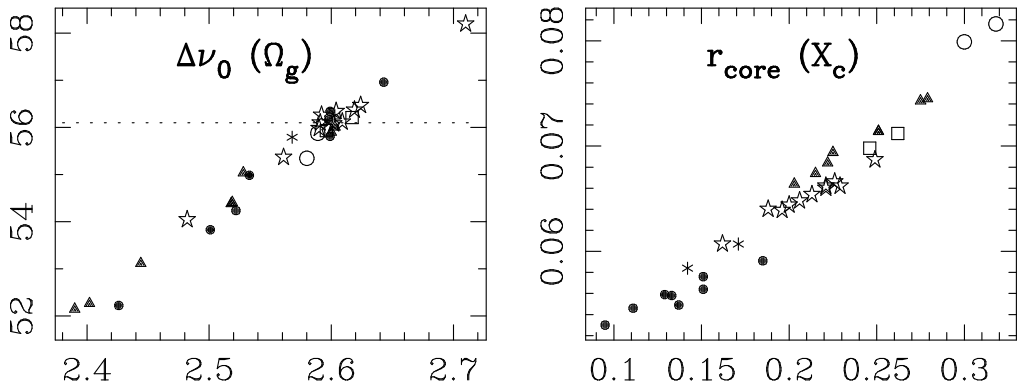

Fig. 10.— Plots of global characteristics quantities for all the stellar models of table 1. The mean frequency spacings are estimated from frequencies computed with Nice2 code. The symbols indicate the values of overshoot parameters ($\zeta = 0.3$ open circle; ζ =0.2 full triangle; ζ =0.15 open square; ζ =0.10 open star; ζ =0.05 * symbol; $\zeta = 0$ full circle). The dotted line corresponds to mean large spacing for the exercise frequency set.

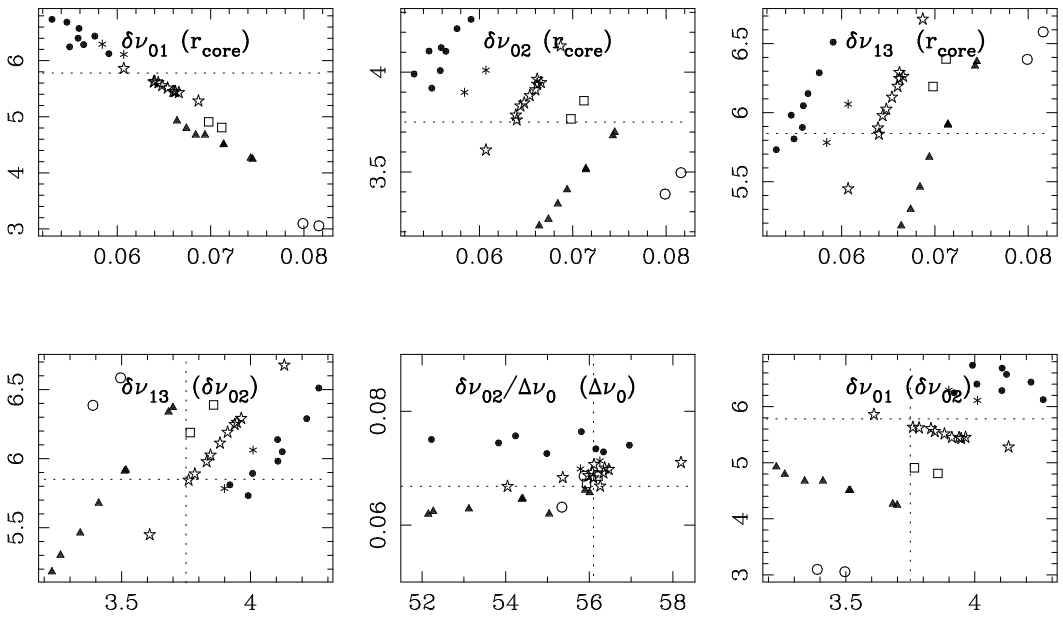

Fig. 11.— Plots of global characteristics quantities for all the stellar models of table 1. The mean frequency spacings are estimated from frequencies computed with Nice2 code. Same symbols as in Fig. 10. The dotted lines indicate the estimated values for the exercise frequency set: $\Delta\nu_0 = 56.1\mu$Hz, $\overline{\delta\nu}_{0,1} = 5.78\mu$Hz, $\overline{\delta\nu}_{0,2} = 3.75\mu$Hz, and $\overline{\delta\nu}_{1,3} = 5.85\mu$Hz.

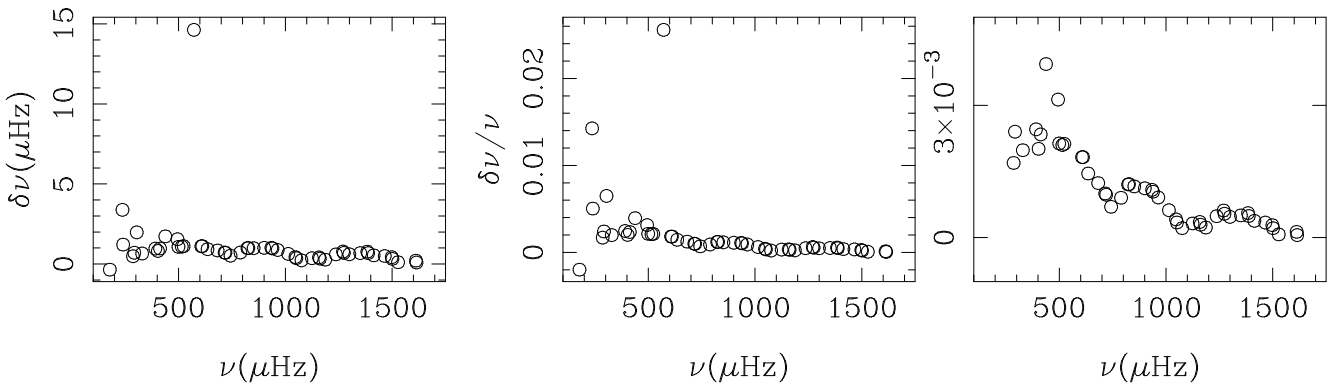

Fig. 12.— Frequency differences, for modes of degree ℓ= 0 to 3, between model E1 and exercise frequency set. Left panel: $\delta\nu$, middle panel $\delta\nu/\nu$, right panel $\delta\nu/\nu$ at a larger scale. In that case $\delta\Omega_g/\Omega_g$ is very small of order 0.1%.

density. At the evolutionary stage of the considered models, the radius of the convective core $r_{\rm core}$ decreases with the age. $r_{\rm core}$ is a function of the central hydrogen content X_c. Figure 10 shows that these two relations do not depend much on the description of the convection, i.e. on the overshoot and mixing-length parameters.

Figure 11 (upper line) shows that, for a given overshoot parameter ζ, there is a well defined relation between the radius of the convective core $r_{\rm core}$ and the mean small spacings $\overline{\delta\nu}_{0,1}$, $\overline{\delta\nu}_{0,2}$ and $\overline{\delta\nu}_{1,3}$. The quantities $\overline{\delta\nu}_{0,2}$ and $\overline{\delta\nu}_{1,3}$ are increasing functions of $r_{\rm core}$. In the range of considered stellar parameters these mean small spacings vary respectively within 1μHz and 1.5μHz. The mean small spacing $\overline{\delta\nu}_{0,1}$ is a decreasing function of $r_{\rm core}$. It is much less dependent on the overshoot parameter and it varies within 2μHz. Thus it seems to be a better indicator of the size of the convective core. The ratio $\overline{\delta\nu}_{0,1}/\overline{\delta\nu}_{0,2}$ is also very sensitive to the size of the convective core (Audard et al. 1995).

Figure 11 (lower line) represents some relations between the different mean frequency spacings which are "observable" quantities. The plots $\overline{\delta\nu}_{1,3}$ ($\overline{\delta\nu}_{0,2}$) or $\overline{\delta\nu}_{0,1}$ ($\overline{\delta\nu}_{0,2}$) show that for a given overshoot parameter the points corresponding to our different models, which have a given chemical composition, are rather well aligned independently on the mass, age and mixing-length parameter. In both plots, the points corresponding to the exercise frequency set are well aligned with models computed with ζ= 0.1.

From the mean large spacing $\Delta\nu_0 \sim 56.1\,\mu$Hz estimated from the exercise frequency set of degree $\ell = 0$, one has $\Omega_g \sim 2.610^{-4}$ (thus $\overline{\rho} \sim 0.16\overline{\rho}_\odot$). If we restrict ourselves to the models of the HR box which have an Ω_g close to this value (denoted by ••), the range of mass and overshoot parameter is limited as follows:

$$(\frac{M}{M_\odot}, \zeta) \sim (1.5, \zeta = 0.3) \rightarrow (1.57, \zeta = 0)$$

Looking at the plots $\overline{\delta\nu}_{1,3}$ ($\overline{\delta\nu}_{0,2}$) or $\overline{\delta\nu}_{0,1}$ ($\overline{\delta\nu}_{0,2}$), we see that the overshoot parameter ζ of the unknown model is around 0.1. Note that, as expected, these plots do not permit to distinguish between models of different values of the mixing-length parameter. These plots indicate a core radius $r_{\rm core} \sim 0.06 - 0.063$.

This radius corresponds to a central hydrogen $\mathrm{X_c} \sim 0.16 - 0.20$.

Models with mean large and small spacings close to that of the exercise can be obtained using different values of the mixing-length parameter λ. For a given mass, models with larger λ have a given Ω_g at a larger age, and thus they correspond to smaller $\overline{\delta\nu}_{0,2}$ and $\overline{\delta\nu}_{1,3}$ and to larger $\overline{\delta\nu}_{0,1}$. Thus among the models we have computed, we have obtained 4 models

$$M/M_\odot = 1.525 \;\; \zeta = 0.1 \;\; \lambda = 1.70, \quad M/M_\odot = 1.525 \;\; \zeta = 0.1 \;\; \lambda = 1.85$$

$$M/M_\odot = 1.530 \;\; \zeta = 0.1 \;\; \lambda = 1.70, \quad M/M_\odot = 1.530 \;\; \zeta = 0.1 \;\; \lambda = 1.80$$

which have values of the small spacings within 0.2 μHz to the exercise values. The $\overline{\delta\nu}_{0,1}$ spacing seems to favour the two models with $\lambda \sim 1.80$.

To go further one has to analyze more in detail the frequencies of the exercise and to compare them with that of these models. This requires to better "calibrate" the models on the mean large spacing $\Delta\nu_0$ value of the exercise ($\Delta\nu_0 \sim 56.1\mu$Hz). Figure 12 shows that the relative frequency differences between the exercise frequency set and the well-calibrated E1 model frequencies are smaller than 10^{-3} for ν larger than 1 mHz. These frequency differences present a well-characterized oscillation which remains to be interpreted. They could be caused by the differences between the oscillatory components due to the HeII ionisation zone. Work is in progress to analyze the behaviour of the second differences $\delta^2\nu_{n,\ell}$ which could inform us on the mixing-length parameter.

In conclusion, this exercise is very preliminary compared to a real stellar case, because the chemical composition is fixed, the range of parameters describing the convection is given and a lot of identified modes with exact frequencies are available. A more realistic case, taking into account a smaller set of frequencies with realistic error bars, will be studied in a next step (see Berthomieu 2000).

REFERENCES

Audard N., Provost J., 1994, A&A 282, 73

Audard N., Provost J., Christensen-Dalsgaard J., 1995, A&A 297, 427

Barban C., Michel E., Martic M., Schmitt J., Lebrun J. C., Baglin A., Bertaux J. L., 1999, A&A 350, 671

Berthomieu G., 2000, these proceedings

Berthomieu G., Provost J., Morel P., Lebreton Y., 1993, A&A 268, 775

Caughlan G. R., Fowler W. A., 1988, Atomic Data an Nuclear Data Tables, 40, 284

Eggleton P.P., Faulkner J., Flannery B. P., 1973, A&A 23, 325

Gough D.O., 1991, Comments on Helioseismic Inference. In: Osaki Y. & Shibahashi H. (eds.) Progress of Seismology of the Sun and Stars, Springer Verlag, 283

Gough D.O., 1998, Inversion for the internal structure and rotation of the Sun and other sun-like stars in: Science with a Small Space Telescope, the First MONS Workshop, held in Aarhus, Denmark, June 29 - 30, 1998, eds.: H. Kjeldsen, T.R. Bedding, Aarhus Universitet, p. 33

Morel P., 1997, A&A S 124, 597

Morel P., Van't Veer C., Provost J., Berthomieu G., Castelli F., Cayrel R., Goupil M.J., Lebreton Y., 1994, A&A 286, 91

Roxburgh I., Vorontsov S.V., 2000, private communication

Unno W., Osaki Y., Ando H., Saio H., Shibahashi H., 1989, Nonradial Oscillations of Stars; University of Tokyo Press

Vorontsov S.V., Zharkov V.N., 1989, Sov. Sci. Rev. E. Astrophys. Space Phys. vol 7, p 1-103